Preprints, 4th IFAC Conference on
Advances in Proportional-Integral-Derivative Control
Almería, Spain | June 12-14, 2024

Nonlinear PID-based temperature control techniques in greenhouses using natural ventilation ⋆

Manuel Berenguel * **Clara Iborra** * **Francisco Rodríguez** *
Francisco García-Mañas * **José Luis Guzmán** *
Jorge A. Sánchez-Molina *

* *University of Almería, CIESOL, ceiA3, Department of Informatics, 04120 Almería, Spain (e-mail: beren@ual.es).*

Abstract: Greenhouses provide controlled environments for cultivating crops. This work explores the design of PID-based greenhouse climate control techniques using natural ventilation, considering both measurable disturbances and operational constraints. A nonlinear model was developed to relate natural ventilation (the primary climate actuator) with interior temperature in greenhouses, the critical factor being the relationship between air flow rate and vent aperture, which is a source of uncertainty in the related literature. Novel calibration issues are included for this term. The nonlinear model is used to devise control strategies combining PI control and feedback linearization. The resulting simulations and robustness analysis, which accounts for uncertainties in the relevant parameters, demonstrate that the combination of PID and feedback linearization techniques is a suitable control approach. In summary, practical tradeoffs can be achieved between setpoint tracking, disturbance rejection, control effort, and robustness.

Keywords: PID control, feedback linearization, greenhouse control, disturbance rejection.

1. INTRODUCTION

Climate control in greenhouses enables optimal crop production. The air temperature inside the greenhouse significantly affects the physiological processes of the plants, and therefore it is important to regulate it in an appropriate range depending on the crop variety and greenhouse location. This controls plant growth and increases the quality of production while reducing energy consumption (Rodríguez et al., 2015; Montoya-Ríos et al., 2020).

The microclimate within a greenhouse is determined by a combination of physical processes that involve the transfer of energy (radiation and heat) and the balance of mass (water vapor and carbon dioxide fluxes). These processes are affected by external environmental conditions, the structure of the greenhouse, the soil material, the type and state of the crop, and the influence of actuators.

The temperature inside a greenhouse regulated by natural ventilation is affected by a variety of factors, such as solar radiation, outside temperature, wind speed, soil temperature, and nonmeasurable disturbances such as crop transpiration. Natural ventilation allows for air exchange between the interior and exterior of the greenhouse. Generally, the outside air is cooler than the inside air and tends to fill the lower layers of the air volume. Warm air rises to the upper layers and exits the greenhouse through the top vents (Rodríguez et al., 2015; Montoya-Ríos et al., 2020).

Algorithms are needed to regulate the indoor temperature by controlling the opening of vents, taking into account the aspects that have been mentioned. The literature on control techniques is vast (García-Mañas, 2023). In relation to those discussed in this work, PID control (Boaventura Cunha et al., 1997; Davis, 1984; Setiawan et al., 1998), event-based control (Liu et al., 2022), feedforward control (García-Mañas et al., 2021; Montoya-Ríos et al., 2020; Rodríguez et al., 2001) and modifications based on feedback linearization (Hoyo et al., 2019; Lijun et al., 2018; Piñón et al., 2005) should be highlighted. PID control compensates for disturbances by feedback. Event-based control allows saving energy at the cost of worsening setpoint tracking. Feedforward control is usually implemented through a static term or by using transfer functions only valid in a determined operating point. This work is based on the combination of PI and feedback linearization techniques, proposing algorithms that allow the temperature in a greenhouse to be regulated throughout the operational range using natural ventilation. The main contribution of the paper is the methodology for calibrating control-oriented models of greenhouse climate, where the relationship between air flow rate and vents aperture is different from that used by other authors, and the analysis and evaluation of different control approaches for this kind of application.

The next section describes the greenhouse from which the data were obtained for model calibration and validation, followed by sections summarizing the models obtained, the control techniques developed, and the simulation results. The paper ends with the main conclusions.

⋆ This work is a result of the CyberGreen Project, PID2021-122560OB-I00, and the Agroconnect (www.agroconnect.es) facilities, grant EQC2019-006658-P, both funded by MCIN/AEI/10.13039/501100011033 and by ERDF A way to make Europe.

2. GREENHOUSE FACILITY

The greenhouse used in this study is illustrated in Figure 1. It is located at El Ejido (Almería, South-East Spain) with a total surface of 1500 m^2 and a volume of 6995 m^3 for growing tomatoes. Data were collected over a period of ten days in August, which is the worst-case scenario for temperature control with natural vents in warm latitudes. Solar radiation and wind speed values were filtered out because of noise in the measurement signal. The sampling time is 1 minute (one test day is 1440 minutes). The ventilation used is the zenithal (top) one. Temperature values inside the greenhouse are very high because of the season of the year. The reason is that during August there is no production in the greenhouse, so new strategies can be tested without impacting on the crop. Notice that not considering the crop is worse for temperature control because the crop is a natural cooler, which favours a drop in temperature. Therefore, if the designed controllers perform well, they will also perform well at any other time of the year when the transpiration of the crop influences the inside temperature.

3. GREENHOUSE TEMPERATURE MODEL

A complete model of the greenhouse climate based on energy and mass balances can be found in (Rodríguez et al., 2015). From the complete model, a simplified lumped-parameter model of greenhouse temperature only considering natural ventilation as actuator is given as follows, where the dependence of variables with time has been omitted for the sake of space:

$$c_t \frac{dX_{t,a}}{dt} = c_r P_{r,e} + c_{cvs}(X_{t,ss} - X_{t,a}) - \\ -(\phi_v + c_{cvc})(X_{t,a} - P_{t,e}) \quad (1)$$

with

$$\phi_v = \frac{c_{d,a} c_{sp,a}}{c_{ga}} \cdot \frac{c_{ven,l} c_{cd}}{3 c_g} \cdot \frac{P_{t,e}}{(X_{t,a} - P_{t,e})} \cdot \\ \cdot \left[\left(\frac{X_{t,a} - P_{t,e}}{P_{t,e}} c_g 2 c_{ven,w} \sin\left(\frac{U}{2}\right) + c_{cvi} P_{v,e}^2 \right)^{\frac{3}{2}} - \left(c_{cvi} P_{v,e}^2\right)^{\frac{3}{2}} \right]$$

where $X_{t,a}$ is the inside temperature (controlled variable, K), U is the manipulated variable (vents aperture, limited between 0° and 31.7°), entering the equation within the ventilation flow term ϕ_v, and $P_{r,e}$ (W/m^2), $P_{t,e}$ (K), $P_{v,e}$ (m/s) and $X_{t,ss}$ (K) are the main disturbances, namely outside radiation, temperature, wind speed and soil temperature, respectively. The effect of crop transpiration is considered an unmeasurable disturbance, as discussed above. There are models in the literature (Rodríguez et al., 2015) in which the latent heat effect of crop transpiration inside the greenhouse is modelled through the leaf area index.

All the values of the coefficients in (1) are defined in Appendix A (note that $c_t = c_{sp,a} c_{d,a} (c_{gv}/c_{ga})$). c_r is the coefficient of absorption of short-wave radiation of the air, c_{cvs} is the coefficient of convection with the soil, c_{cvc} is the coefficient of heat transfer through the greenhouse cover due to convection and conduction effects (loss coefficient), c_{cvi} is the wind effect coefficient, which

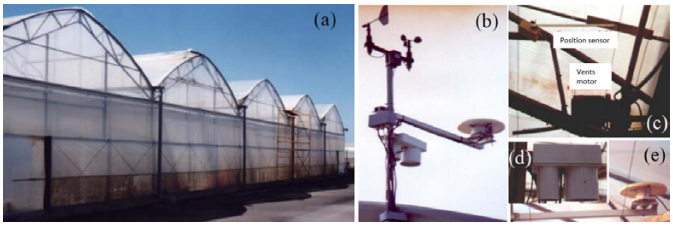

Fig. 1. (a) Greenhouse, (b) outdoor weather station, (c) detail of top ventilation, (d) temperature and humidity sensor and (e) indoor radiation sensor

considers the effects due to the pressure differences caused by the wind, and c_{cd} is the discharge coefficient, which is a ratio of the theoretical flow rate to the actual flow rate flowing through the ventilation openings. These last two coefficients depend on wind speed, so considering them as constants introduces uncertainty in the model. More details on these coefficients can be found in Rodríguez et al. (2015).

3.1 Model calibration

Some of these coefficients must be estimated using real data. As the model is nonlinear, genetic algorithms (Houck et al., 1996) were used to determine the values of these parameters, based on minimization of the mean square error ($MSE = \frac{1}{N}\sum_{k=1}^{N}(y(k) - y_m(k))^2$, y being the real temperature and y_m that provided by the model). In addition, to assess the model fitting, comparison statistics are used, such as the mean (MAE) and maximum absolute error (MxAE), as well as its standard deviation (StAE). The search ranges for the parameters were established based on those published in the literature and a previous calibration in (Rodríguez et al., 2015), which has been improved following the proposed methodology, where it has been taken into account that three of the coefficients are not related to ventilation ($c_r \in [0.04\ 0.5], c_{cvs} \in [0.5\ 3], c_{cvc} \in [1\ 5]$) while two of them play a relevant role in the ventilation flux ($c_{cvi} \in [0.08\ 1], c_{cd} \in [0.1\ 1]$). Therefore, a two-stage calibration procedure was used, first estimating the three parameters that do not depend on ventilation (using data when the vents are fully closed - stage 1) and once their value was fixed, those related to ventilation are estimated on days when the vents are opened (stage 2). Figure 2 (top plot) shows the days used in stage 1 and stage 2. This two-stage approach also takes into account the results of the sensitivity analysis explained in the next subsection, from which it was concluded that the main parameters that influence model calibration are c_r and c_{cvc}, which are fixed in the first stage. For calibration, 80% of the available data in each stage (without and with ventilation) is used to find the best solutions with genetic algorithms, and the remaining 20% is used to validate the model with the new estimated parameters (including a day with and a day without ventilation). In the genetic algorithm, as combination operators, simple and heuristic crossover and crossover arithmetic were used, while as mutation operators nonuniform and boundary mutation were chosen. The final values for the model parameters found are shown in Appendix A. Compared to the values previously estimated in (Rodríguez et al., 2015), the improvements can be seen in Table 1. Figure 3 shows the performance of

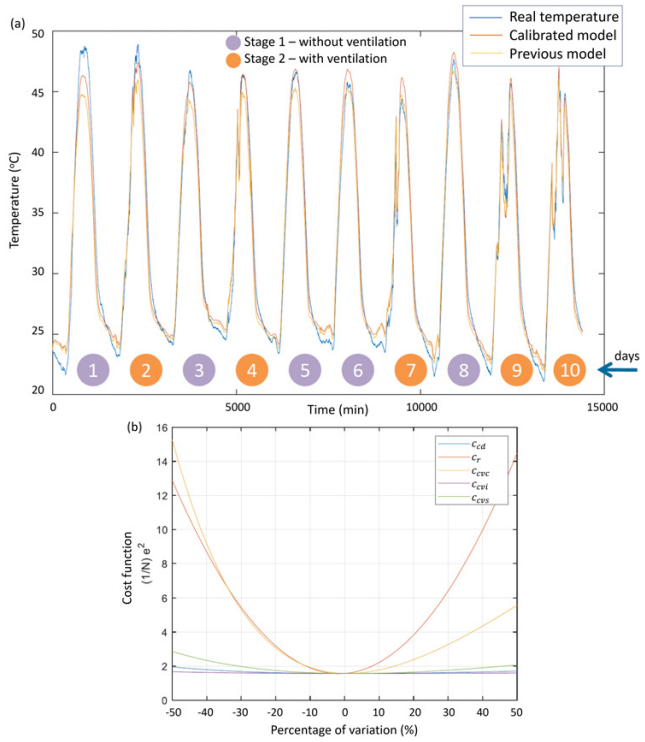

Fig. 2. (a) stages of the calibration procedure and final validation results with all the data. (b) plot of the sensitivity analysis

the calibrated model in two days, one without ventilation and the other with ventilation.

Table 1. Statistics on the total data

	MSE	MAE	MxAE	StAE
Initial parameters	2.9350	1.3487	5.0427	1.0566
Final parameters	1.6574	1.0735	3.3524	0.7107

3.2 Sensitivity analysis

Sensitivity analysis is a tool that helps calibrate models and consists of measuring the degree to which variations in one or several parameters affect the fitting of the model to real data. The procedure is as follows: the value of a parameter is modified in a range around its established value, theoretically the optimum, in such a way that small variations are made successively until the whole range is covered; for each of these variations, the model is evaluated. The evaluation criterion would coincide with the selection function to be optimized. Once the whole model has been evaluated for the range of parameter variations, the results of the evaluation of the cost function against the parameter variations are plotted and analyzed. This process can be repeated for all parameters to be analyzed by setting all parameters to their fixed value except for the one under study. Figure 2 (lower plot) shows a plot of the results of the sensitivity analysis. Note that there is symmetry in the evaluation of the cost function with respect to the minimum, which confirms the hypothesis of using MSE.

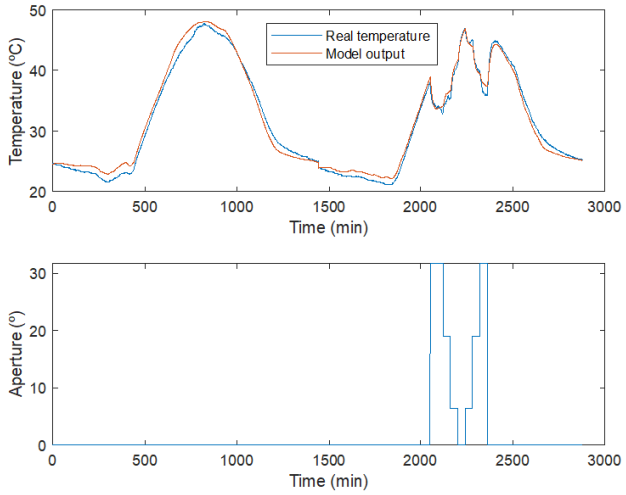

Fig. 3. Results of the calibration procedure

4. CONTROL APPROACHES

Based on (1), different control approaches can be proposed considering PID control and modifications. Feedforward control can be used in this kind of plant (Rodríguez et al., 2001). For example, linearization of (1) around a particular operating point provides the transfer functions that relate the inputs (both controllable ones and disturbances) to the output. The linearization procedure is included in Appendix B (online). Substituting the values of the descriptive parameters of the model leads to the linearized differential equation, which allows simplified transfer functions relating the inputs (manipulable and disturbances) to the output to be obtained. The transfer functions that relate the disturbances to the output allow for the design of feedforward controllers. This control approach has shown to provide adequate results, but it is sensitive to modelling uncertainties and provides different closed-loop performance (in terms on characteristics response times) depending on the operating conditions (for that reason, results are not shown in this paper due to space restrictions).

In this paper, PID-based feedback linearization is used to control the greenhouse, as explained in the following.

4.1 Nonlinear PI-based control with feedback linearization

This control approach seeks to achieve good disturbance rejection while maintaining the same closed-loop behaviour even when changes in operating conditions occur. The feedback linearization technique (Isidori, 1995) is based on the idea of treating nonlinear systems as linear ones (through algebraic transformations and feedback), which can then be controlled with PID control schemes. As the relative degree of the nonlinear model in (1) is one and there is a direct relationship between the manipulable variable and the controlled one, feedback linearization (FL) can be applied by replacing different terms (always including nonlinear ones) to the right of the equal sign with a virtual control signal $v(t)$, making the system linear (either an integrator $G(s) = k/s$ or a first order $G(s) = k/(\tau s + 1)$) and allowing for the use of PI controllers for design purposes. The relationship between

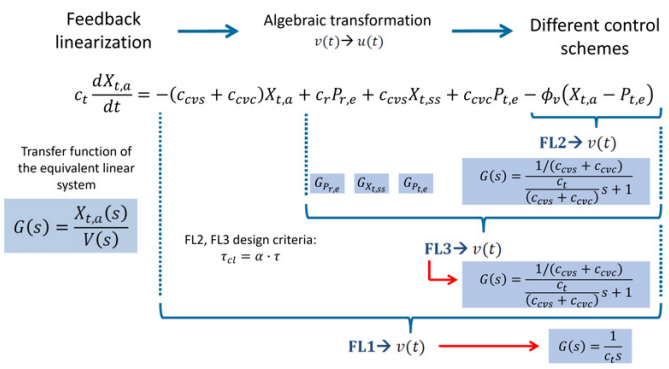

Fig. 4. Selection of $v(t)$ in FL1, FL2 and FL3

the virtual control signal $v(t)$ and the real control signal $U(t)$ is algebraic and invertible under logical operational assumptions (e.g. there is no thermal inversion). This approach is easy to implement, but requires constraint mapping mechanisms, which means that the saturation in the control signal $U(t)$ is transformed to time-varying limits in the virtual control signal $v(t)$, that is,

$$v_{min}(t) = \min_{U_{min} \le U(t) \le U_{max}} v(t),$$
$$v_{max}(t) = \max_{U_{min} \le U(t) \le U_{max}} v(t). \quad (2)$$

The different design approaches (FL1, FL2, and FL3) are shown in Figure 4, depending on the choice of virtual control signal $v(t)$. Table 2 summarizes the main equations used for the design of the controllers. For PI design purposes using the linear equivalent, the specification has been $\tau_{cl} = \alpha\tau$, providing $K_c = 1/(\alpha k_U)$. The parameter α is selected equal to 0.2 in the simulations shown in this paper. The tracking constant of the anti-windup mechanism is selected as $T_t = T_i$. The implementation is also described in Figure 5. The relationship between the virtual control signal $v(t)$ and the real control signal $U(t)$ is given in Table 3. As can be seen, this nonlinear transformation is invertible in every case where there is no thermal inversion, that is, the indoor temperature is different from the outdoor temperature (usually higher). Operational constraints in v or U (2) can be imposed to avoid U reaching large values. Note that if in the third method (FL3), instead of using pole-zero cancelation, the SIMC method is applied (Skogestad, 2003), it provides $T_i = 0.8\tau$ as the only difference, providing quite acceptable results (FL3.2). Figure 6 shows representative results with the four approaches.

4.2 Evaluation of the control approaches

In addition to the well-known IAE ($\int |e(t)|dt$), ITAE ($\int |te(t)|dt$), ISE ($\int e^2(t)dt$), and ITSE ($\int te^2(t)dt$) indexes used to evaluate controller performance based on the error between reference and output ($e(t) = r(t) - y(t)$), the Control Effort Index $CEI = \int |\Delta u(t)|$ has also been used (Table 4). The best controller is FL1, with lower control effort and better performance. However, a robustness analysis considering uncertainties in c_r, c_{cvc} and c_{cvs} (performing variations of $\pm 10\%$ about nominal values) reflects that FL1 is in this case less robust against model uncertainties and prone to large settling times, as the controller does not include integral action, which is also a problem when load disturbances are present. The analysis has been performed using four days with extreme values in the performance indices selected to cover the maximum range of possible behaviours and the average indices obtained are shown in Table 5. For example, when variations in c_r are produced, FL1 varies the nominal indices between 96% and 134%, while the other approaches do so in a narrower interval (90% to 113%). FL3 (in each of the options) is the best solution according to the results in Table 4 and the robustness analysis.

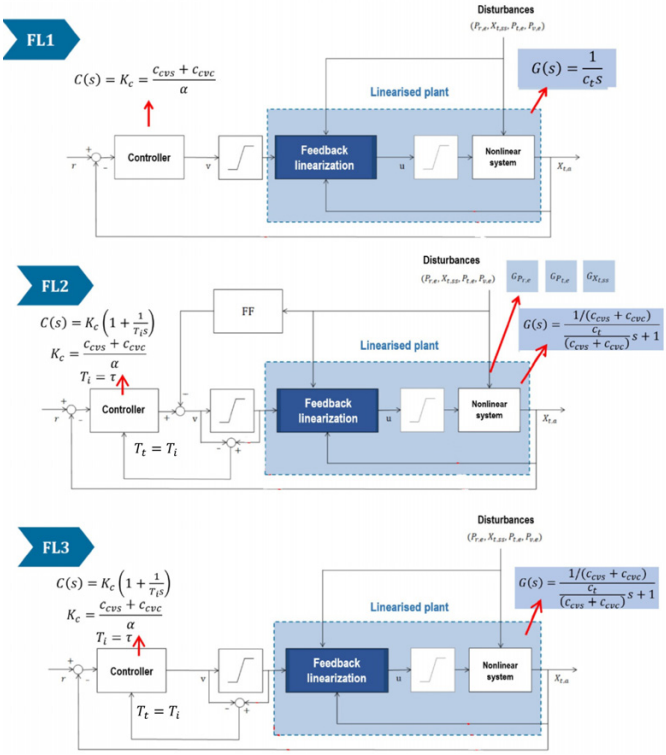

Fig. 5. Nonlinear PI based on FL approaches

Table 2. Summary of controllers' design

	FL1
Virtual signal	$v = c_r P_{r,e} + c_{cvs}(X_{t,ss} - X_{t,a}) -$ $-(\phi_v + c_{cvc})(X_{t,a} - P_{t,e})$
Linear equivalent	$G(s) = 1/(c_t s)$; $k = 1.782 \cdot 10^{-4}$ Km^2/J
Controller	$C(s) = K_c$, $K_c = 29.48$ J/(Km^2)
Closed loop	$G_{cl} = 1/((c_t/K_c)s + 1)$; $\tau_{cl} = 3.17$ min
	FL2
Virtual signal	$v = -\phi_v(X_{t,a} - P_{t,e})$
Linear equivalent	$G(s) = \gamma/(c_t\gamma s + 1)$, $\gamma = 1/(c_{cvs} + c_{cvc})$ $k = 0.17$ Km^2/W; $\tau = 15.86$ min
Controller	$C(s) = K_c(1 + 1/(T_i s))$, $T_t = T_i$; $K_c = 29.48$ W/(Km^2); $T_i = 15.86$ min
Feedforward	$F_{ffP_{r,e}}(s) = -c_r$; $F_{ffX_{t,ss}} = -c_{cvs}$; $F_{ffP_{t,e}} = -c_{cvc}$
Closed loop	same as FL1
	FL3
Virtual signal	$v = c_r P_{r,e} + c_{cvs} X_{t,ss} + c_{cvc} P_{t,e} -$ $-\phi_v(X_{t,a} - P_{t,e})$
Linear equivalent	same as FL2
Controller	same as FL2
Closed loop	same as FL2
FL3.2, SIMC	$C(s) = K_c(1 + 1/(T_i s))$, $T_t = T_i$; $K_c = 29.48$ W/(Km^2); $T_i = 12.68$ min

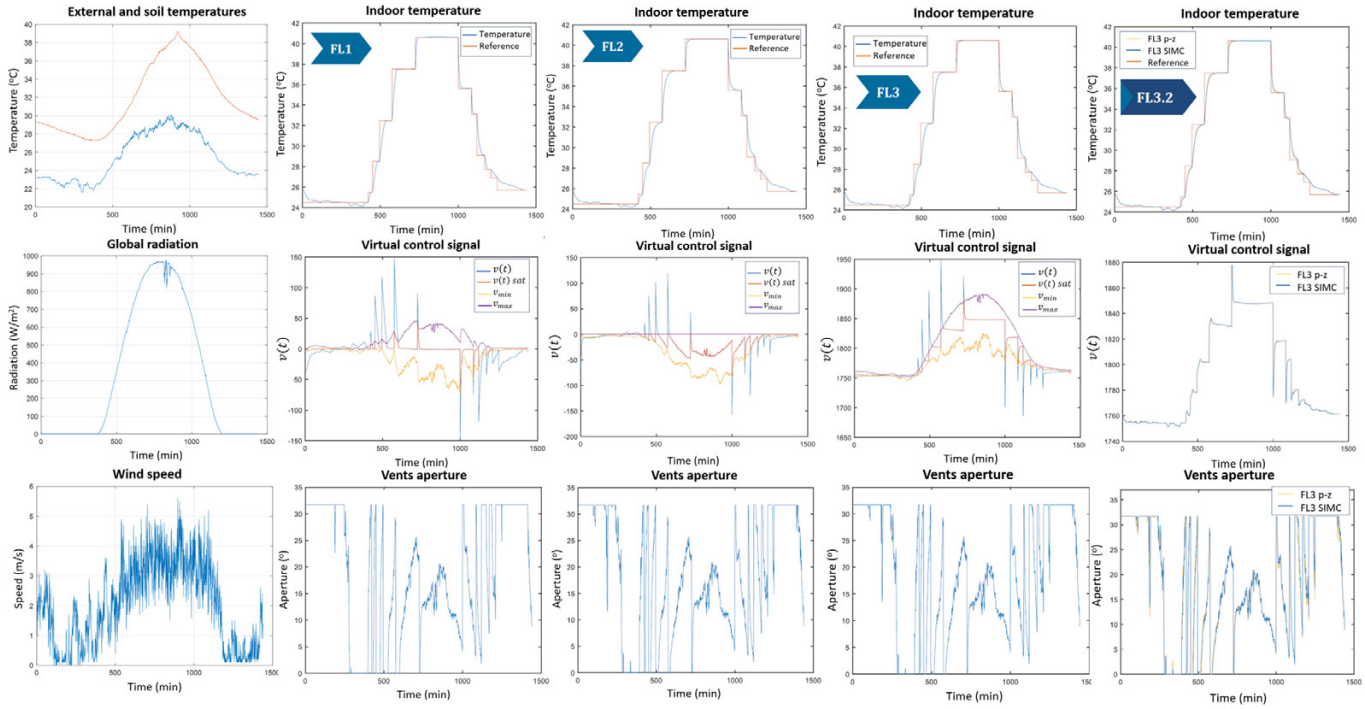

Fig. 6. Simulation results. The first column shows the main disturbances, the other columns show the performance achieved with FL1, FL2, FL3 and FL3.2, respectively

Table 3. Relationships between U and v, with $c_1 = \left(\frac{c_{sp,a}c_{d,a}}{c_{ga}}\right) \cdot \left(\frac{c_{ven,l}c_{cd}}{3c_g}\right)$, $c_2 = 2c_g c_{ven,w}$

FL1:	$U = 2\arcsin\left[\left(\left(\frac{c_r P_{r,e}+c_{cvs}X_{t,ss}+c_{cvc}P_{t,e}-(c_{cvs}+c_{cvc})X_{t,a}-v}{c_1 P_{t,e}} + (c_{cvi}P_{v,e}^2)^{\frac{3}{2}}\right)^{\frac{2}{3}} - c_{cvi}P_{v,e}^2\right)\frac{P_{t,e}}{(X_{t,a}-P_{t,e})}\frac{1}{c_2}\right]$
FL2:	$U = 2\arcsin\left[\left(\left(\frac{-v}{c_1 P_{t,e}} + (c_{cvi}P_{v,e}^2)^{\frac{3}{2}}\right)^{\frac{2}{3}} - c_{cvi}P_{v,e}^2\right)\frac{P_{t,e}}{(X_{t,a}-P_{t,e})}\frac{1}{c_2}\right]$
FL3:	$U = 2\arcsin\left[\left(\left(\frac{c_r P_{r,e}+c_{cvs}X_{t,ss}+c_{cvc}P_{t,e}-v}{c_1 P_{t,e}} + (c_{cvi}P_{v,e}^2)^{\frac{3}{2}}\right)^{\frac{2}{3}} - c_{cvi}P_{v,e}^2\right)\frac{P_{t,e}}{(X_{t,a}-P_{t,e})}\frac{1}{c_2}\right]$

Table 4. Performance and control effort indices for all designed controllers

	IAE	ISE	ITAE	ITSE	CEI
FL1	372.81	562.72	268610	405443	1145.69
FL2	417.40	607.32	300738	437578	1266.91
FL3	416.33	606.40	299960	436913	1265.70
FL3.2	390.48	584.28	281523	420970	1231.97

5. CONCLUSIONS

This article introduces an enhanced nonlinear model of a greenhouse, which has been refined through the implementation of a parameter calibration approach that relies on stepwise data decomposition and sensitivity analysis. Although the amount of data available has been a limitation, the methodology is extensible to any type of greenhouse. Different types of controller that combine PID control with feedback linearization have been developed and compared in simulation. Various metrics have been used in the comparison and an analysis of the robustness to uncertainty has been conducted. It was found that the first controller, whose transfer function is an integrator, gave a better response and a slightly more favourable control effort, but did not respond well in the face of uncertainty. The FL3 approaches appear to be suitable for this kind of application, as they achieve a good tradeoff between performance and robustness against model uncertainty. As the controller includes integral action, steady-state errors are avoided even in the presence of uncertainty.

The control strategy can be implemented using the discrete-time version of the nonlinear model and a sampling time appropriate to closed-loop dynamics (at least 1/10 of the closed-loop time constant). Notice that the final user only has to modify the desired closed-loop time constant once implemented to modify performance; this is also another advantage of the approach. Future work will include the extension of the proposed methodology to the simultaneous control of temperature and humidity, also using the nonlinear model that relates humidity to

natural ventilation and a selective control algorithm, as presented in (García-Mañas et al., 2024). In real tests, it will be analyzed if it is necessary to include any model adaptation or robustification mechanism as in (Guesbaya et al., 2022), but from the robustness analysis it seems not necessary.

Table 5. Indices in the robustness analysis

Parameter	IAE	ISE	ITAE	ITSE	CEI
FL1					
$c_r(-10\%)$	498.67	671.97	359285	484153	1097.55
$c_r(+10\%)$	473.09	549.91	340683	396210	1152.49
$c_{cvc}(-10\%)$	430.07	570.80	316295	411220	1117.41
$c_{cvc}(+10\%)$	412.97	585.12	297540	421583	1122.27
$c_{cvs}(-10\%)$	370.39	545.64	266868	393133	1156.05
$c_{cvs}(+10\%)$	404.35	590.99	291342	425805	1096.11
FL2					
$c_r(-10\%)$	452.23	684.42	325825	493130	1218.00
$c_r(+10\%)$	395.72	547.27	285135	394308	1281.14
$c_{cvc}(-10\%)$	419.92	598.32	302550	431088	1294.72
$c_{cvc}(+10\%)$	427.55	624.31	308053	449820	1204.23
$c_{cvs}(-10\%)$	410.08	592.77	295460	427103	1244.22
$c_{cvs}(+10\%)$	438.29	630.93	315778	454575	1266.91
FL3					
$c_r(-10\%)$	450.89	682.96	333373	492078	1217.00
$c_r(+10\%)$	394.62	546.46	284323	393725	1279.82
$c_{cvc}(-10\%)$	420.18	497.86	302743	430758	1231.36
$c_{cvc}(+10\%)$	424.65	622.68	305948	448635	1251.08
$c_{cvs}(-10\%)$	407.02	591.33	293258	426048	1288.89
$c_{cvs}(+10\%)$	437.59	630.22	315278	454075	1203.29
FL3.2					
$c_r(-10\%)$	424.81	659.25	306075	474985	1180.79
$c_r(+10\%)$	372.45	528.76	268348	380973	1250.26
$c_{cvc}(-10\%)$	394.56	577.05	284283	415765	1205.08
$c_{cvc}(+10\%)$	400.12	601.25	291200	433195	1209.29
$c_{cvs}(-10\%)$	381.58	569.72	274975	410483	1255.80
$c_{cvs}(+10\%)$	395.09	586.86	296823	439268	1168.95

ACKNOWLEDGEMENTS

Author Francisco García-Mañas was supported by an FPU grant from the Spanish Ministry of Science, Innovation, and Universities.

REFERENCES

Boaventura Cunha, J., Couto, C., and Ruano, A. (1997). Real-time parameter estimation of dynamic temperature models for greenhouse environmental control. *Control Engineering Practice*, 5(10), 1473–1481. doi:10.1016/S0967-0661(97)00145-7.

Davis, P. (1984). A technique of adaptive control of the temperature in a greenhouse using ventilator adjustments. *Journal of Agricultural Engineering Research*, 29(3), 241–248. doi:10.1016/0021-8634(84)90101-X.

García-Mañas, F. (2023). *Automatic Control Strategies for Optimal Economic and Energy Management of Greenhouse Crop Production*. PhD Thesis, University of Almería.

García-Mañas, F., Guzmán, J.L., Rodríguez, F., Berenguel, M., and Hägglund, T. (2021). Experimental evaluation of feedforward tuning rules. *Control Engineering Practice*, 114, 104877. doi:10.1016/j.conengprac.2021.104877.

García-Mañas, F., Hägglund, T., Guzmán, J.L., Rodríguez, F., and Berenguel, M. (2024). A practical solution for multivariable control of temperature and humidity in greenhouses. *European Journal of Control*, 77, 100967. doi:10.1016/j.ejcon.2024.100967.

Guesbaya, M., García-Mañas, F., Megherbi, H., Rodríguez, F., and Berenguel, M. (2022). Real-time adaptation of a greenhouse microclimate model using an online parameter estimator based on a bat algorithm variant. *Computers and Electronics in Agriculture*, 192, 106627. doi:10.1016/j.compag.2021.106627.

Houck, C., Joines, J., and Kay, M. (1996). *A genetic algoritm for function optimization: A Matlab implementation*. NCSU-IE Technical Report 9509; North Carolina State University, USA.

Hoyo, A., Moreno, J.C., Guzmán, J.L., and Rodríguez, F. (2019). Robust QFT-based feedback linearization controller of the greenhouse diurnal temperature using natural ventilation. *IEEE Access*, 7, 64148–64161. doi:10.1109/ACCESS.2019.2916412.

Isidori, A. (1995). *Nonlinear control systems (3rd ed.)*. Springer.

Lijun, C., Shangfeng, D., Meihui, L., and Yaofeng, H. (2018). Adaptive feedback linearization-based predictive control for greenhouse temperature. *IFAC-PapersOnLine*, 51(17), 784–789. doi:10.1016/j.ifacol.2018.08.100.

Liu, R., Guzmán, J.L., García-Mañas, F., and Li, M. (2022). Selective temperature and humidity control strategy for a chinese solar greenhouse with an event-based approach. *Revista Iberoamericana de Automática e Informática industrial*, 20(2), 150–161. doi:10.4995/riai.2022.18119.

Montoya-Ríos, A.P., García-Mañas, F., Guzmán, J.L., and Rodríguez, F. (2020). Simple tuning rules for feedforward compensators applied to greenhouse daytime temperature control using natural ventilation. *Agronomy*, 10(9). doi:10.3390/agronomy10091327.

Piñón, S., Camacho, E.F., Kuchen, B., and Peña, M. (2005). Constrained predictive control of a greenhouse. *Computers and Electronics in Agriculture*, 49(3), 317–329. doi:10.1016/j.compag.2005.08.007.

Rodríguez, F., Berenguel, M., and Arahal, M.R. (2001). Feedforward controllers for greenhouse climate control based on physical models. In *2001 European Control Conference (ECC)*, 2158–2163. doi:10.23919/ECC.2001.7076243.

Rodríguez, F., Berenguel, M., Guzmán, J.L., and Ramírez-Arias, A. (2015). *Modeling and control of greenhouse crop growth*. Springer:Cham, Switzerland. doi:10.1007/978-3-319-11134-6.

Setiawan, A., Albright, L.D., and Phelan, R.M. (1998). Simulation of greenhouse air temperature control using PI and PDF algorithms. *IFAC Proceedings Volumes*, 31(12), 111–117. doi:10.1016/S1474-6670(17)36050-0.

Skogestad, S. (2003). Simple analytic rules for model reduction and PID controller tuning. *Journal of Process Control*, 13(4), 291–309. doi:10.1016/S0959-1524(02)00062-8.

Appendix A. MAIN PARAMETERS OF THE MODEL

Parameter	Symbol	Value	Units
Radiation coefficient	c_r	0.0911	-
Soil convection coefficient	c_{cvs}	2.3769	W/(m^{2}K)
Cover convection coefficient	c_{cvc}	3.5195	W/(m^{2}K)
Wind effect coefficient	c_{cvi}	0.7630	-
Discharge coefficient	c_{cd}	0.1327	-
Length of ventilation	$c_{ven,l}$	40	m
Width of ventilation	$c_{ven,w}$	1.9250	m
Acceleration of gravity	c_g	9.8	m/s^2
Air density	$c_{d,a}$	1.197	kg/m^3
Specific heat of air	$c_{sp,a}$	1005	J/(kgK)
Greenhouse area	c_{ga}	1500	m^2
Greenhouse volume	c_{gv}	6995	m^3

Appendix B. LINEARIZATION OF THE MODEL

Linearization of the model can be found in

`https://cutt.ly/TwSef2yT`